HHS Public Access

Author manuscript

Nat Med. Author manuscript; available in PMC 2015 September 01.

Published in final edited form as:

Nat Med. 2015 March ; 21(3): 248–255. doi:10.1038/nm.3806.

A small molecule inhibitior of the NLRP3 inflammasome is a potential therapeutic for inflammatory diseases

Rebecca C. Coll[1,2], **Avril A. B. Robertson**[2], **Jae Jin Chae**[3], **Sarah C. Higgins**[1], **Raúl Muñoz-Planillo**[4], **Marco C. Inserra**[2,5], **Irina Vetter**[2,5], **Lara S. Dungan**[1], **Brian G. Monks**[6], **Andrea Stutz**[6], **Daniel E. Croker**[2], **Mark S. Butler**[2], **Moritz Haneklaus**[1], **Caroline E. Sutton**[1], **Gabriel Núñez**[4], **Eicke Latz**[6], **Daniel L. Kastner**[3], **Kingston H. G. Mills**[1], **Seth L. Masters**[7], **Kate Schroder**[2], **Matthew A. Cooper**[2], and **Luke A. J. O'Neill**[1]

[1]School of Biochemistry and Immunology, Trinity Biomedical Sciences Institute, Trinity College Dublin, Dublin 2, Ireland [2]Institute for Molecular Bioscience, University of Queensland, Brisbane, Australia [3]Inflammatory Disease Section, Medical Genetics Branch, National Human Genome Research Institute, National Institutes of Health, Bethesda, Maryland 20892, USA [4]Department of Pathology and Comprehensive Cancer Center, University of Michigan Medical School, Ann Arbor, MI 48109, USA [5]School of Pharmacy, The University of Queensland, Brisbane, Australia [6]Institute of Innate Immunity, University Hospitals, Biomedical Centre, University of Bonn, Bonn, Germany [7]The Walter and Eliza Hall Institute of Medical Research, Parkville 3052, Australia

Abstract

The NLRP3 inflammasome is a component of the inflammatory process and its aberrant activation is pathogenic in inherited disorders such as the cryopyrin associated periodic syndromes (CAPS) and complex diseases such as multiple sclerosis, type 2 diabetes and atherosclerosis. We describe the development of MCC950, a potent, selective, small molecule inhibitor of NLRP3. MCC950 blocks canonical and non-canonical NLRP3 activation at nanomolar concentrations. MCC950 specifically inhibits NLRP3 but not AIM2, NLRC4 or NLRP1 activation. MCC950 reduces Interleukin-1p (IL-1β) production *in vivo* and attenuates the severity of experimental autoimmune encephalomyelitis (EAE), a disease model of multiple sclerosis. Furthermore, MCC950 treatment rescues neonatal lethality in a mouse model of CAPS and is active in *ex vivo* samples from

Corresponding author Correspondence to: L. A. J. O'Neill or M. A. Cooper.

Author Contributions

R.C.C. performed and analysed the experiments in Fig 1b–j, Fig 2, Fig 3a,b, Fig 4f–h and Supplementary Fig. 6b–g, helped analyse the experiments in Fig. 5a–c and Supplementary Fig. 6h,i and wrote the manuscript. A.A.B.R. synthesised MCC950, conducted formulation for *in vivo* studies, determined compound pharmacokinetics, helped write the manuscript and provided advice. J.J.C performed the experiments in Fig. 6f and Supplementary Fig. 8. S.C.H performed and analysed the experiment in Fig. 5d–g. R.M.P performed the experiments in Fig. 4a,b M.C.I and I.V performed the experiments in Fig. 4c–e. L.S.D performed the experiment in Fig. 5a–c. B.G.M and A.S performed the experiments in Fig. 3c and Supplementary Fig 7. D.E.C performed the experiments in Supplementary Fig. 6a. M.S.B performed the NMR analysis in Supplementary Fig. 1–5 and Supplementary Table 1. M.H performed the experiments in Supplementary Fig. 6h,i. C.E.S helped analyse data from the experiment in Fig. 5d–g. S.L.M performed and analyzed the experiments in Fig. 6a–e. G.N., D.K.L. and E.L. oversaw a portion of the work. K.H.G.M conceived ideas and oversaw a portion of the work. K.S, S.L.M. and M.A.C. conceived ideas, oversaw a portion of the work, reviewed the manuscript and provided advice. L.A.J.O. conceived ideas oversaw the research programme and wrote the manuscript

Competing financial interests

The authors declare no competing financial interests.

individuals with Muckle-Wells syndrome. MCC950 is thus a potential therapeutic for NLRP3-associated syndromes, including autoinflammatory and autoimmune diseases, and a tool for the further study of the NLRP3 inflammasome in human health and disease.

Introduction

The NOD-like receptor family (NLR) protein NLRP3 is an intracellular signalling molecule that senses many pathogen-, environmental- and host-derived factors[1]. Upon activation NLRP3 binds to apoptosis associated speck-like protein containing a CARD (ASC). ASC in turn interacts with the cysteine protease caspase-1, forming a complex termed the inflammasome. This results in the activation of caspase-1, which cleaves the pro-inflammatory cytokines IL-1β and IL-18 to their active forms and mediates a type of inflammatory cell death known as pyroptosis[2]. Other intracellular pattern recognition receptors (PRRs) are also capable of forming inflammasomes. These include other NLR family members such as NLRP1 and NLRC4 and non-NLR PRRs such as the double-stranded DNA (dsDNA) sensors absent in melanoma 2 (AIM2) and interferon, gamma inducible protein 16 (IFI16)[3]. NLRP3-dependent IL-1β processing can also be activated by an indirect, non-canonical pathway downstream of caspase-11[4]

The inherited CAPS Muckle-Wells syndrome (MWS), familial cold autoinflammatory syndrome (FCAS) and neonatal onset multi-system inflammatory disease (NOMID) are caused by gain of function mutations in NLRP3, thus defining NLRP3 as a critical component of the inflammatory process[5]. NLRP3 has also been implicated in the pathogenesis of a number of complex diseases, notably metabolic disorders such as type 2 diabetes, atherosclerosis, obesity and gout[6]. A role for NLRP3 in diseases of the central nervous system is emerging, while lung diseases have also been shown to be influenced by NLRP3[7]. Furthermore, NLRP3 plays a role in the development of liver disease[8], kidney disease[9] and aging[10]. Many of these associations were defined using *Nlrp3*$^{-/-}$ mice but there have also been insights into the specific activation of NLRP3 in these diseases. In type 2 diabetes the deposition of islet amyloid polypeptide (IAPP) in the pancreas activates NLRP3 and IL-1β signalling resulting in β-cell death and inflammation[11].

Current treatments for NLRP3 related diseases include biologic agents that target IL-1. These are the recombinant IL-1 receptor antagonist Anakinra, the neutralizing IL-1β antibody Canakinumab and the soluble decoy IL-1 receptor Rilonacept. This has proven successful in the treatment of CAPS and these biologic agents have been subject to clinical trials for other IL-1β associated diseases[12]. Several small molecules have been shown to inhibit the NLRP3 inflammasome. Glyburide inhibits IL-1β production at micromolar concentrations in response to NLRP3 but not NLRC4 or NLRP1 activation[13]. We previously described a small molecule capable of inhibiting both NLRP3 and AIM2 at micromolar concentrations. This molecule was initially incorrectly termed CRID3 but was in fact a Bayer compound that is a cysteinyl leukotriene receptor antagonist[14]. Other purported NLRP3 inhibitors include parthenolide[15], 3,4-methylenedioxy-β-nitrostyrene (MNB)[16] and dimethyl sulfoxide (DMSO)[17], although these agents have limited potency and are non-specific.

In 2001 a number of diarylsulfonylurea-containing compounds were identified as novel IL-1β processing inhibitors[18]. In this study we have investigated one of these we have termed MCC950[19]. The synthesis and chemical structure of MCC950 are described in the methods section, in Supplementary Table 1 and Supplementary Fig.1–5. Here, we describe how MCC950 is a highly potent specific NLRP3 inhibitor, which is active *in vivo* in multiple NLRP3-dependent mouse models and in *ex vivo* samples from individuals with CAPS.

Results

MCC950 inhibits both canonical and non-canonical NLRP3 activation

The effect of MCC950 (Fig. 1a) on NLRP3 inflammasome activation was tested in mouse bone marrow derived macrophages (BMDM), human monocyte derived macrophages (HMDM) and human peripheral blood mononuclear cells (PBMC). Cells were first primed with LPS then pre-treated with MCC950 and lastly stimulated with the NLRP3 stimulus ATP. Treating cells with nanomolar concentrations of MCC950 dose dependently inhibited the release of IL-1β in BMDM (Fig. 1b), HMDM (Supplementary Fig. 6a) and PBMC (Supplementary Fig. 6b. The half-maximal inhibitory concentration (IC_{50}) of MCC950 in BMDM was approximately 7.5 nM, while in HMDM it had a similar inhibitory capacity (IC_{50} = 8.1 nM). LPS-dependent tumor necrosis factor-α (TNF-α) secretion was not impaired by MCC950 (Fig. 1b and Supplementary Fig. 6a,b) demonstrating that the inhibition of IL-1β secretion was specific.

The amount of caspase-1 p10 (an auto-processed fragment of caspase-1) was dose-dependently reduced in supernatants from MCC950-treated BMDM and PBMC (Fig. 1c and Supplementary Fig. 6c), suggesting MCC950 inhibits the activation of caspase-1 by NLRP3. Correspondingly, the processing of IL-1β was inhibited by MCC950 (Fig. 1c and Supplementary Fig. 6c). MCC950 treatment did not consistently affect the expression of pro-IL-1β or pro-caspase-1 in cell lysates (Fig. 1c and Supplementary Fig. 6c). Similarly, treatment with glyburide inhibited caspase-1 activation and IL-1β processing in these assays (Fig. 1c and Supplementary Fig. 6c).

We also tested MCC950 with other NLRP3 stimuli. LPS primed BMDM were treated with MCC950 and stimulated with the ionophore nigericin[20] (Fig. 1d–g) or monosodium urate crystals (MSU)[21] (Supplementary Fig. 6d–g). MCC950 inhibited IL-1β release in response to both stimuli (Fig. 1d and Supplementary Fig 6d) but did not block TNF-α secretion (Fig. 1e and Supplementary Fig. 6g). IL-1α and lactate dehydrogenase (LDH) release induced by nigericin were potently blocked by MCC950 (Fig. 1 f, g) but MCC950 did not block IL-1α or LDH in response to MSU (Supplementary Fig. 6e,f). It was previously demonstrated that MSU induced IL-1α and LDH release is NLRP3 independent[22,23]. The effects of MCC950 on IL-1α and LDH release (Fig. 1f,g and Supplementary Fig. 6e,f) thus suggest that MCC950 specifically blocks NLRP3-dependent pyroptotic cell death. In contrast to short-term stimulation with LPS (3 h), PBMC seeded at high density and stimulated with LPS alone for 24 h activate caspase-1 and secrete IL-1β due to endogenous ATP release[24]. We found that MCC950 also dose dependently inhibited IL-1β but not TNF-α secretion in this assay (Supplementary Fig. 6h,i).

Gram-negative bacteria and intracellular LPS are sensed by a non-canonical pathway, resulting in caspase-11-dependent pyroptotic cell death and IL-1β production[4]. NLRP3 is required for IL-1β processing by the non-canonical pathway[25, 26]. We activated caspase-11 in BMDM primed with the TLR2/1 ligand Pam3CSK4 and transfected with LPS[26] (Fig 1h–j). Using *Casp11*$^{-/-}$ and *Nlrp3*$^{-/-}$ BMDM we confirmed that IL-1β secretion is dependent on both NLRP3 and caspase-11 and that LDH and IL-1α release are not dependent on NLRP3 in this assay (Fig. 1h–j). We found that pre-treatment of wild-type (WT) cells with MCC950 prior to transfection with LPS resulted in a dose-dependent inhibition of IL-β release (Fig. 1h) but had no effect on IL-1α secretion (Fig. 1i) or LDH release (Fig. 1j). MCC950 thus specifically blocks caspase-11-directed NLRP3 activation and IL-1β secretion upon stimulation of the non-canonical pathway.

MCC950 does not inhibit NLRC4, AIM2, NLRP3 priming or TLR signaling

Next we examined whether MCC950 could inhibit the activation of other inflammasome complexes. NLRC4-stimulated IL-1β and TNF-α secretion (as activated by *Salmonella typhimurium*[27]) were not inhibited by MCC950 even at a concentration of 10 μM (Fig. 2a). MCC950 did not inhibit caspase-1 activation or IL-1β processing in response to *S. typhimurium* (Fig. 2b). The expression of pro-caspase-1 and pro-IL-1β in cell lysates was not substantially affected by MCC950 treatment (Fig. 2b). Parthenolide has previously been shown to inhibit NLRC4 dependent caspase-1 activation[15], although it did not do so in these experiments (Fig. 2b). Parthenolide attenuated IL-1β and TNF-α secretion (Fig. 2a) and also pro-IL-1β expression (Fig. 2b) suggesting its inhibitory effect is on the Nuclear factor-κB pathway rather than on caspase-1 activation by NLRC4.

The effect of MCC950 on the non-NLR AIM2 inflammasome was examined by transfecting BMDM with the dsDNA analogue Poly(dA:dT)[28–31]. MCC950 treatment did not attenuate IL-1β or TNF-α secretion from BMDM in response to stimulation with LPS and Poly(dA:dT) (Fig. 2c). However, IL-1β but not TNF-α secretion was inhibited in cells treated with a Bayer cysteinyl leukotriene receptor antagonist 1-(5-carboxy-2{3-[4-(3-cyclohexylpropoxy)phenyl]propoxy}benzoyl)piperidine-4-carboxylic acid, as has been previously described[14] (Fig. 2c). The Bayer compound, but not MCC950, inhibited Poly(dA:dT) stimulated caspase-1 activation (Fig. 2d).

We then specifically examined whether MCC950 influenced the priming phase of NLRP3 activation. BMDM were pre-treated with MCC950 or parthenolide and then stimulated with TLR ligands (Fig. 2e,f). As shown in Fig. 2e the LPS stimulated induction of NLRP3 and pro-IL-1β was not affected by MCC950 pre-treatment. Likewise, MCC950 did not affect LPS- or Poly(A:U)-induced TNF-α secretion (Fig. 2f). In contrast parthenolide, which is an inhibitor of IκB Kinase-β (IKK-β)[32] abrogated both TLR4- and TLR3-stimulated TNF-α production. Together these data demonstrate that MCC950 does not inhibit TLR signalling or the priming phase of NLRP3 activation.

MCC950 blocks NLRP3 induced ASC oligomerization

We next examined the formation of NLRP3 dependent ASC oligomers, a key event in NLRP3 inflammasome activation. Similar to results with ATP stimulated cells (Fig. 1c)

MCC950 and glyburide inhibited nigericin induced caspase-1 and IL-1β processing (Fig. 3a) MCC950 did not alter the expression of pro-caspase-1, pro-IL-1β or ASC in cell lysates (Fig. 3a). Cytosolic fractions from cell lysates were cross-linked and ASC monomers and higher order complexes were observed after stimulation with LPS and nigericin. ASC-complex formation was attenuated by MCC950 and glyburide (Fig. 3a). ASC oligomerization was also observed using immortalized macrophages stably expressing cerulean fluorescent protein tagged ASC. Upon NLRP3 activation by ATP the cerulean-ASC condenses into a large speck in each cell (Fig. 3b). Pre-treatment with MCC950 inhibited speck formation (Fig. 3b). The relatively high concentration of MCC950 required to block speck formation in the assay may be due to the nature of the cell line that also stably expresses high levels of NLRP3 and thus does not require priming. ASC-cerulean cells were examined using a range of inflammasome ligands (Fig. 3c and Supplementary Fig. 7). The number of activated cells observed after stimulation with nigericin or the lysosomal destabiliser LeuLeu-OMe which activates NLRP3[33] was dose dependently decreased by pre-treatment with MCC950. Speck formation was not decreased by MCC950 in cells stimulated with the NLRP1 ligand lethal toxin[34] indicating the selectivity of MCC950 for NLRP3 (Fig. 3c and Supplementary Fig. 7).

MCC950 does not block K^+ efflux, Ca^{2+} flux or NLRP3-ASC interactions

We next sought to address the mechanism of action of MCC950. K^+ efflux is a trigger common to all NLRP3 activators[35] and MCC950 is structurally related to sulfonylurea drugs such as glyburide that are known to target ATP-sensitive K^+ channels[36]. MCC950 dose dependently inhibited IL-1β release induced by nigericin, ATP and SiO_2 in LPS primed macrophages, but did not prevent K^+ efflux triggered by these stimuli (Fig. 4a,b). It has been previously demonstrated that NLRP1 inflammasome activation is blocked by high concentrations of extracellular K^+[37] and we found that MCC950 does not block NLRP1 activation (Fig. 3c). These data suggest that MCC950 inhibits NLRP3 activation downstream of K^+ efflux.

A requirement for Ca^{2+} signaling in the activation of NLRP3 was previously demonstrated[38]. We examined whether MCC950 altered ATP induced Ca^{2+} flux (Fig. 4c–e). *Ice*$^{-/-}$ BMDM were tested as caspase-1 activation can lead to nonspecific membrane permeation and Ca^{2+} flux. Pre-treatment with MCC950 in WT or *Ice*$^{-/-}$ BMDM did not substantially affect the ATP induced increase in intracellular Ca^{2+} (Fig. 4c–e), suggesting MCC950 is unlikely to inhibit NLRP3 activation by modulating Ca^{2+} flux.

As we had observed that MCC950 could prevent NLRP3-induced ASC oligomerization we next tested whether MCC950 could prevent direct NLRP3-NLRP3 or NLRP3-ASC interactions (Fig. 4f–h). HEK293T cells were transfected with NLRP3 and ASC, treated with 50 μM MCC950 and then a co-immunoprecipitation assay with NLRP3 was performed. MCC950 did not alter the interaction between NLRP3 with NLRP3 (Fig. 4f lanes 4 and 5) or NLRP3 with ASC (Fig. 4g lanes 4 and 5). We also employed a FACS based assay to analyze GFP–tagged ASC speck formation induced by NLRP3 expression in a ligand independent manner (Fig. 4h). Micromolar doses of MCC950 did not decrease the percentage of ASC speck containing cells. Although we cannot rule out that MCC950 interacts directly with

NLRP3, these data suggest that it does not prevent inflammasome formation by directly blocking NLRP3 oligomerization or NLRP3-ASC interactions.

MCC950 inhibits NLRP3 *in vivo* and attenuates EAE severity

We next investigated the effects MCC950 *in vivo*. The induction of IL-1β by intraperitoneal (i.p.) injection of LPS was shown to be NLRP3 dependent[39]. We thus examined whether MCC950 could block this induction of IL-1β. Mice were pre-treated with MCC950 one hour before i.p. injection of LPS and were assessed two hours later (Fig. 5a–c). Pre-treatment with MCC950 reduced serum concentrations of IL-1β and IL-6 while it did not considerably decrease the amount of TNF-α, indicating that MCC950 is active *in vivo*.

The effect of MCC950 in animal models of NLRP3 mediated diseases was then tested. EAE is a mouse model of the human disease MS. EAE is induced by immunization with a CNS auto-antigen and causes T cell mediated inflammation and demyelination. IL-1 signalling is crucial to the induction of IL-17 production from pathogenic $CD4^+$ Th17 and $\gamma\delta^+$ T cells[40–42]. More recently it has been demonstrated that the development of EAE requires NLRP3[43]. We investigated the possibility that MCC950 may suppress T cell responses that mediate autoimmune disease. Treatment of mice with MCC950 delayed the onset and reduced the severity of EAE (Fig. 5d). Intracellular cytokine staining and FACS analysis of brain mononuclear cells from mice sacrificed on day 22 showed modestly reduced frequencies of IL-17 and IFN-γ producing $CD3^+$ T cells in MCC950 treated mice in comparison with PBS-treated mice (Fig. 5e). IFN-γ and particularly IL-17 producing cell numbers were also reduced in both the $CD4^+$ and $\gamma\delta^+$ sub-populations of $CD3^+$ T cells (Fig. 5f,g).

MCC950 rescues a mouse model of CAPS and inhibits NLRP3 in human MWS cells

A mouse model of the human CAPS disease MWS was generated by expression of the MWS associated mutation *Nlrp3*^{A350VneoR} (corresponding to NLRP3A352V in humans) specifically in the myeloid lineage (crossed with *LysMCre*)[44]. MWS mice die in the neonatal period and have increased concentrations of circulating IL-1β and IL-18[44]. We treated MWS mice with MCC950 (Fig. 6a) and observed that they had increased body weight at day 9 compared to PBS treated controls (Fig. 6a and 6b). MCC950 also increased survival up to day 38–45 even after treatment was stopped at day 28 (Fig. 6c,d). MCC950 treatment also decreased the concentration of circulating IL-18 in MWS mice; however, IL-18 then increased after the withdrawal of MCC950 (Fig. 6e). A mouse strain containing an Nlrp1 activating mutation (*Nlrp1a*^{Q593P}) also displays increased concentrations of serum IL-18 relative to WT controls[45]. However, treatment of NLRP1 mutant mice with MCC950 did not significantly alter serum concentrations of IL-18 (Fig. 6e) ($P = 0.7$). These data clearly demonstrate that MCC950 effectively and specifically blocks NLRP3 activation *in vivo*.

Finally we tested the effects of MCC950 in PBMC from individuals with MWS, a CAPS caused by gain of function mutations in NLRP3[46]. PBMC from individuals with MWS secrete IL-1β in response to LPS alone without an NLRP3 stimulus[47, 48]. When PBMC from an individual with MWS were stimulated with LPS, caspase-1 and IL-1β processing were detected in the cell supernatants (Fig. 6f). However, when pre-treated with MCC950 both

IL-1β and caspase-1 processing were dose dependently inhibited (Fig. 6f). MCC950 treatment did not alter the expression of pro-IL-1β or pro-caspase-1 (Fig. 6f). Samples from four more individuals with MWS were also found to be sensitive to MCC950 inhibition (Supplementary Fig. 8). Thus, MCC950 inhibits inflammasome activation in samples from individuals with CAPS.

In vitro and *in vivo* pharmacokinetics of MCC950

To assess the therapeutic potential of MCC950, the pharmacokinetic profile of this compound was examined in a number of *in vitro* absorption, distribution, metabolism and excretion assays. The stability of MCC950 when incubated with human or mouse liver microsomes was good with more than 70% of the compound remaining after 60 min (Supplementary Table 2). The drug-drug interaction potential of MCC950 was also tested (Supplementary Table 3, 4). MCC950 was incubated at a single concentration of 10 μM with human liver microsomes and a cocktail of standard substrates specific for each of the 5 major cytochrome P450 (CYP) isozymes (1A2, 2C9, 2C19, 2D6 and 3A4). The inhibition of the 5 major CYP enzymes with MCC950 was low at less than 15% (Supplementary Table 4). In order to explore any potential for cardiotoxicity, the effect of MCC950 on the human ether-a-go-go (hERG) potassium channel was examined using the high throughput automated patch clamp method ($QPatch^{HTX}$) (Supplementary Table 5). In this assay the IC_{50} for hERG was greater than 30 μM suggesting MCC950 has >3,000 fold selectivity window (IC_{50} for NLRP3 = <10 nM). Finally, a single dose pharmacokinetic profile of MCC950 in C57Bl/6 mice was determined via intravenous (3 mg/kg) and oral (20 mg/kg) administration (Supplementary Fig. 9). The area under the curve was 163,410 ng.h/mL with a C_{max} of 25,333 ng/mL and half-life of 3.27 hours. The oral bioavailability of MCC950 was 68%.

Discussion

We describe here MCC950, a potent selective NLRP3 inhibitor that is active both in mice *in vivo* and in human cells *ex vivo*. MCC950 may be a useful tool to explore NLRP3 biology and druggability.

We have characterised the mechanism of action of MCC950 within our current understanding of NLRP3 activation. MCC950 did not block K^+ efflux, Ca^{2+} flux or ligand independent direct NLRP3 and ASC interactions. Reactive oxygen species (ROS) have been implicated but current evidence suggests that ROS are not involved in NLRP3 activation by nigericin or ATP[38,49], which are both potently inhibited by MCC950. As MCC950 is active against the hypersensitive NLRP3 mutations in MWS, against non-canonical NLRP3 activation and against all tested canonical NLRP3 stimuli this suggests that its molecular target of MCC950 is NLRP3 itself or is closely linked to the activation of NLRP3. It is possible that MCC950 binds to NLRP3 and affects a key step in its activation that might involve post-translational modification. Future work will aim to define the precise mechanism of action of MCC950.

We note that targeting NLRP3 might present certain advantages over biologic inhibitors of IL-1β. MCC950 had a dramatic effect on a genetic mouse model of CAPS. The rescue

afforded by MCC950 is far more substantial than the targeted blockade of IL-1β alone, which does not prevent lethality[44]. Some of the pathology of this disease may be due to IL-18 and pyroptosis[50], which MCC950 will block. IL-1β maturation can be mediated by a number of different enzymes including serine proteases and caspase-8[3] and we have demonstrated that MCC950 does not block the major anti-microbial inflammasomes NLRC4 and NLRP1. Thus, specific targeting of NLRP3 will not result in the complete blockade of IL-1β *in vivo* during infection and antimicrobial responses may remain intact. MCC950 may therefore have less immunosuppressive effects when compared to biologics such as Canakinumab, which has been shown clinically to increase the risk of these serious infections[12,51]. MCC950 will also have a shorter half-life compared to the biologics Canakinumab and Rilonacept, and can therefore be withdrawn should unwanted effects occur such as infections. A small molecule such as MCC950 may also be more cost effective than biologic agents[52]. The future clinical development of MCC950 or derivatives may result in the development of new anti-inflammatory therapies for CAPS, but also more complex diseases such as type 2 diabetes, MS and Alzheimer's disease.

Methods

MCC950 synthesis and formulation

MCC950 was synthesised *via* a 10 step route[53]. The 1,2,3,5,6,7-hexahydro-s-indacen-4-amine moiety was synthesised from 2,3-dihydro-1H–indene where Friedel-Craft's acylation using 3-chloropropionyl chloride and aluminium trichloride in dichloromethane gave 3-chloro-1-(2,3-dihydro-1H-inden-5-yl)propan-1-one which was not purified but used directly in the cyclisation reaction. Cyclisation was achieved by heating the crude product to 60 °C in concentrated sulphuric acid for 72 h then the solution was cooled to 0 °C and nitrated directly using a 1:1 mixture of nitric and sulphuric acids. After trituration with ice cold methanol a regio-isomeric mixture of 4-nitro and 8-nitro-3,5,6,7-tetrahydro-s-indacen-1(2H)-one was isolated in 61% yield over the three synthetic steps. Simultaneous reduction of the ketone and nitro groups was successfully achieved by hydrogenation in methanol over Pearlman's catalyst in the presence of methanesulfonic acid in 62% yield after purification by column chromatography on silica.

The required 4-(2-hydroxypropan-2-yl)furan-2-sulfonamide moiety was synthesised from ethyl furan-3-carboxylate. Sulfonylation of the furan 5 position was readily achieved using chlorosulfonic acid in dichloromethane at –10 °C to room temperature. The 4-(ethoxycarbonyl)furan-2-sulfonic acid intermediate was not isolated but chlorinated directly by addition of pyridine then phosphorous pentachloride to the reaction mixture. After work-up and silica column chromatography ethyl 5-(chlorosulfonyl)furan-3-carboxylate was isolated in 56% yield over the two steps. The chloride was displaced using ammonium bicarbonate in water and acetone to yield 4-(2-hydroxypropan-2-yl)furan-2-sulfonamide in 59% yield after aqueous work-up. The sulphonamide was pure enough to use in the next reaction step where the ester moiety was reduced, using methylmagnesium chloride in tetrahydrofuran, to the tertiary alcohol giving 4-(2-hydroxypropan-2-yl)furan-2-sulfonamide in 53% yield.

To complete the synthesis of MCC950 the 1,2,3,5,6,7-hexahydro-s-indacen-4-amine was converted to the corresponding isocyanate by reaction with di-tbutyldicarbonate and N,N-dimethylaminopyridine in acetonitrile. The sodium salt of 4-(2-hydroxypropan-2-yl)furan-2-sulfonamide was prepared by reaction with freshly prepared sodium methoxide solution and the solvent removed *in vacuo* to give a hygroscopic sodium salt. The salt was suspended in acetonitrile, the preformed isocyanate solution added and the reaction stirred overnight. MCC950 sodium salt was filtered directly from the reaction mixture and the beige solid was triturated using ethyl acetate. The product was dissolved in water, treated with activated charcoal and filtered through celite. The aqueous solution was freeze dried to give the desired product as the sodium salt.

Spectra of MCC950 and intermediates are consistent with literature precedent[53] and HRMS (ESI) calculated for MCC950 C20H23N2O5S (M-H+) 403.1333, found 403.1351. MCC950 sodium salt is highly soluble in aqueous solutions and therefore was formulated in saline for *in vivo* studies.

Cell culture

Bone marrow from C57BL/6, *Nlrp3*$^{-/-}$ (Martinon et al.[21]), *Ice*$^{-/-}$ (Kuida et al.[54] and *Casp11*$^{-/-}$ (Wang et al.[55]) mice was differentiated for 7 days in DMEM supplemented with 10% fetal calf serum (FCS), 1% penicillin/streptomycin (P/S) and 20% L929 mouse fibroblast supernatant or in RPMI 1640 medium supplemented with 10% FCS, 1% P/S and 10 ng/ml human M-CSF (ImmunoTools). Stably transfected ASC-cerulean macrophages as described by Hett et al.[56] were a kind gift from Dr. Eicke Latz, University of Bonn, Germany, and were cultured in DMEM supplemented with 10% FCS and 1% P/S. HEK293T cells were cultured in DMEM supplemented with 10% FCS and 1% P/S. Blood specimens from individuals with CAPS were drawn after obtaining informed consent under a protocol approved by the NIAMS/NIDDK Institutional Review Board. Human PBMC were isolated by LSM-Lymphocyte Separation Medium (50494, MP Biomedicals) from freshly drawn peripheral venous blood. PBMC were cultured in RPMI 1640 medium containing 10% FCS and antibiotics. HMDM were generated from CD14^{+} monocytes by differentiation for 7 days in IMDM supplemented with 10% FCS, 1% P/S and 10 ng/ml human M-CSF (Miltenyl Biotec) as described by Croker et al.[57]

Inflammasome activation assays

BMDM were seeded at 5 ×$_0$ 10^5/ml or 1 × 10^6/ml, HMDM at 5 × 10^5/ml and PBMC at 2 × 10^6/ml or 5 ×$_0$ 10^6/ml in 96 well plates. The following day the overnight medium was replaced and cells were stimulated with 10 ng/ml LPS from Escherichia coli serotype EH100 (ra) TLRgrade™ (Alexis Biochemicals) for 3 h. Medium was removed and replaced with serum free medium (SFM) containing DMSO (1:1,000), MCC950 (0.001–10 μM), glyburide (200 μM) (Sigma Aldrich), parthenolide (10 μM) (Enzo Life Sciences) or Bayer cysteinyl leukotriene receptor antagonist 1-(5-carboxy-2{3-[4-(3-cyclohexylpropoxy)phenyl]propoxy}benzoyl)piperidine-4-carboxylic acid (40 μM) (Amgen Inc., Thousand Oaks, CA, USA) for 30 min. Cells were then stimulated with inflammasome activators: 5 mM adenosine 5'-triphosphate disodium salt hydrate (ATP) (1 h), 1 μg/ml Poly(deoxyadenylic-thymidylic) acid sodium salt (Poly dA:dT) (Sigma Aldrich) transfected

with Lipofectamine 2000™ (Invitrogen) (3–4 h), 200 μg/ml MSU (overnight) and 10 μM nigericin (Invivogen) (1 h) or *S. typhimurium* UK-1 strain (M.O.I. 20) obtained from Dr. Sinead Corr, Trinity College Dublin, Ireland (2 h). Cells were also stimulated with 25 μg/ml Polyadenylic-polyuridylic acid (Invivogen) (4 h). For non-canonical inflammasome activation cells were primed with 100 ng/ml Pam3CSK4 (Invivogen) for 4 h, medium was removed and replaced with SFM containing DMSO or MCC950 and 2 μg/ml LPS was transfected using 0.25% FuGENE® (Promega) for 16 h. Supernatants were removed and analysed using ELISA kits according to the manufacturer's instructions (DuoSet® R&D Systems or ReadySetGo!® eBioscience). LDH release was measured using the CytoTox96® non-radioactive cytotoxicity assay (Promega)

Western blotting

Cell lysates were prepared by direct lysis in 50 μl 5 ⅄ Laemmli sample buffer. The protein content of supernatants was concentrated using StrataClean™ resin (Agilent Technologies) according to the manufacturer's instructions. The protein samples were resolved on 15% SDS-PAGE gels and transferred onto polyvinylidene diflouride (PVDF) membrane using a wet transfer system. Membranes were blocked in 5% (w/v) dried milk in TBS-T (50 mM Tris/HCL, pH 7.6, 150 mM NaCl and 0.1% (v/v) Tween-20) for 1 h at room temperature (RT). Membranes were incubated with primary antibody diluted in 5% (w/v) dried milk in TBS-T, followed by incubation with the appropriate horseradish peroxidise (HRP) conjugated secondary antibody diluted in 5% (w/v) dried milk in TBS-T for 1 h. Membranes were developed using 20 ⅄ LumiGLO® chemilluminescent reagent (Cell Signaling Technology). Membranes were stripped using Restore™ PLUS western blot stripping buffer (Thermo Fisher Scientific) before being reprobed.

PBMC from individuals with CAPS were seeded at $2 \times_0 10^6$/ml in 12 well plates and then primed with 1 μg/ml LPS for 3 h. Medium was replaced with SFM containing MCC950 (5–1,000 nM). After 45 min, cell culture supernatants and cell lysates were collected. Samples were resolved using Novex® Tris-Glycine Gel Systems (Invitrogen).

Primary antibodies used were: ASC antibody (AL177) (1 in 1,000) (Enzo Life Sciences), β-actin (AC-74) (1:10,000), FLAG M2 (F1804) (1:2,500) and α-Tubulin clone B-5-1-2 (T5168) (1:5,000) (Sigma Aldrich), Mouse caspase-1 p10 (sc-514) (1:1,000), human caspase-1 p10 (sc-515) (1:1,000), human pro-caspase-1 (sc-622) (1:1,000) and human actin (sc-1615) (1:1,000) (Santa Cruz Biotechnology), mouse IL-1β (AB-401-NA) (1:1,000) and human IL-1β (AF-201-NA) (1:1,000) (R&D Systems), HA.11 clone 16B12 (MMS-101R) (1:2,000) (Covance), NLRP3 clone Cryo-2 (AG-20B-0014) (1:1,000) (Adipogen). Secondary HRP conjugated antibodies were: anti-mouse IgG, anti-rabbit IgG and anti-goat IgG (all 1:1,000) (Jackson ImmunoResearch Inc.).

ASC complex isolation

BMDM were seeded at 10^6/ml in 6 well plates. The following day medium was replaced and cells were stimulated with 10 ng/ml LPS for 3 h. Medium was removed and replaced with SFM containing the indicated inhibitors or controls for 30 min, followed by the addition of 10 μM nigericin for 1 h. The supernatants were removed, cells were rinsed in ice-cold PBS

and 500 μl ice-cold buffer (20 mM Hepes-KOH, pH 7.5, 150 mM KCL, 1%NP-40 0.1 mM PMSF, 1 mg/ml leupeptin, 11.5 mg/ml aprotinin and 1 mM sodium orthovanadate) was added. Cells were scraped and lysed by shearing 10 ✓ through a 21 gauge needle. 50 μl of lysate was removed for Western blot analysis. Lysates were centrifuged at 330 × g for 10 min at 4 °C. The pellets were washed twice in 1 ml ice-cold PBS and resuspended in 500 μl PBS. 2 mM disuccinimydyl suberate (from a fresh 100 mM stock prepared from DSS equilibrated to RT and made up in dry DMSO) was added to the re-suspended pellets, which were incubated at RT for 30 min with rotation. Samples were then centrifuged at 330 × g for 10 min at 4 °C. The supernatant was removed and the cross-linked pellets were resuspended in 30 μl Laemmli sample buffer. Samples were boiled for 5 min at 99 °C and analysed by Western blotting.

Confocal microscopy

For confocal images ASC-cerulean cells were seeded at 2×10^5/ml the day prior to use in experiments on 35 mm glass bottom culture dishes. The following day the overnight medium was replaced with SFM containing the indicated inhibitors or controls for 30 min. Cells were then stimulated with 5 mM ATP for 30 min. Imaging was performed on an Olympus FluoView™ FV1000 Microscope equipped with a temperature and CO^2 controlled chamber. For quantification of ASC speck formation ASC-cerulean cells were seeded at 3.75×10^5/ml the day prior to use in experiments in 384 well plates. The following day MCC950 was added using a HP compound printer, 1 h later activators were added: 10 μM nigericin (1.5 h), 1 mM LeuLeuOMe (2 h) and 1 μg/ml lethal toxin (1 μg/ml lethal factor plus 1 μg/ml protective antigen - 2 h). A solution of DRAQ5 (1:1,000) and 1% formaldehyde were added and the plates were quantitated as described in Hett et al[56].

K^+ analysis

Intracellular K^+ measurements were performed by inductively coupled plasma optical emission spectrometry (ICP-OES) with a PerkinElmer Optima 2000 DV spectrometer using yttrium as internal standard as described by Mũnoz-Planillo et al.[35] Cells were stimulated with 500 ng/ml LPS for 3 h, treated with MCC950 (10–300 nM) and then stimulated with 10 μM nigericin or 5 mM ATP for 30 min or 375 μg/ml SiO_2 for 6 h

Fluorescent Imaging Plate Reader (FLIPR) Ca^{2+} analysis

BMDM (3×10^4/well) were loaded for 30 min at 37 °C with a no wash calcium dye (Molecular Devices) in physiological salt solution (PSS; composition NaCl 140 mM, glucose 11.5 mM, KCl 5.9 mM, $MgCl_2$ 1.4 mM, NaH_2PO_4 1.2 mM, NaHCO3 5 mM, CaCl2 1.8 mM, HEPES 10 mM) containing 0.1% BSA. Cells were then transferred to the $FLIPR^{TETRA}$ (Molecular Devices) fluorescent plate reader and Ca^{2+} responses measured using a cooled CCD camera with excitation at 470–495 nM and emission at 515–575 nM. Camera gain and intensity were adjusted for each plate to yield a minimum of 1,000 arbitrary fluorescence units (AFU) baseline fluorescence. Prior to addition of MCC950, 10 baseline fluorescence readings were taken, followed by fluorescent readings every second for 300 seconds following sample addition and a further 300 seconds following addition of either PSS or ATP (500 μM).

Co-immunoprecipitation assay

HEK293T cells (3×10^5 /ml) were transfected in 10 cm^2 dishes by calcium phosphate method with the following plasmids: pEF6 mouse NLRP3 N-HA, pEF6 mouse ASC, pEF6 mouse NLRP3 N-FLAG or empty vector control. 24 h post transfection cells were lysed in RIPA buffer (50 mM Tris-HCL pH8, 150 mM NaCL, 1 mM EDTA, 10% Glycerol, 1% Triton X-100, 1% Sodium deoxycholate, 0.1% SDS and protease inhibitors) and disrupted by passage through a 27G needle. Lysates were precleared with 5 μl protein G Dynabeads (Life Techonologies) for 30 min at 4°C. Dynabeads were blocked in 0.5% BSA for 1 h at 4°C. Lysates were incubated for 1 h with 0.5 μg anti-FLAGM2 (F1804) (Sigma-Aldrich) antibody before addition of 20 μl blocked Dynabeads for a further 2 h at 4°C. Dynabeads captured using a magnet, washed and resuspended in 60 μl sample buffer and boiled for 5 min before analysis by Western blotting.

Time of Flight Imflammasome Evaluation (TOFIE) assay

HEK293T cells (4×10^5 /ml) were transfected in 24 well plates using Lipofectamine 2000™ (Invitrogen) with the following plasmids: pEF6 human ASC-GFP, pEF6 human C-mCherry or empty vector control. 1 h post transfection cells were treated with DMSO or MCC950 (0.1–50 μM). 15 h post transfection cells were removed and suspended in DPBS containing 1% FCS and 2 mM EDTA. Cells were analysed using a Gallios™ flow cytometer (Beckman Coulter) and using FlowJo software. Live cells were gated on GFP and Cherry expression (when co-transfected). The percentage of ASC speck containing cells was determined by analysing the height and width of the GFP pulse area (low width:area and high height:area). This analysis is described in detail in by Sester et al.[58]

In vivo LPS challenge

C57BL/6 mice were injected intraperitoneally (i.p.) with 50 mg/kg MCC950 or vehicle control (DMSO/PBS) 1 **h** h before i.p. injection of 10 mg/kg LPS Escherichia coli 055:B5 (Sigma Aldrich) or PBS. After for 2 h mice were sacrificed and serum levels of IL-1β, TNF-α and IL-6 were measured by ELISA.

Induction and Assessment of EAE

C57BL/6 mice were immunized subcutaneously with 150 μg of MOG peptide 35–55 (GenScript) emulsified in CFA containing 4 mg/ml (0.4.mg/mouse) of heat-killed MTB (Chondrex). Mice were injected i.p. with 500 ng pertussis toxin (PT: kaketsuken) on days 0 and 2. MCC950 was administered i.p. to mice (10 mg/kg) at induction of the disease, day 0, 1 and 2 and every 2 days thereafter. Control mice were administered vehicle (PBS) at the same time points. Mice were observed for clinical signs of disease daily (unblinded). Disease severity was scored as follows: no clinical signs, 0; limp tail, 1; ataxic gait, 2; hind limb weakness, 3; hind limb paralysis, 4; and tetra paralysis, 5., Experiments were performed under license (BI00/2412) from The Irish Medicine Board and with approval from the Trinity College Dublin BioResources Ethics Committee.

FACS analysis of EAE

On day 22 post immunization mononuclear cells were isolated from whole brains of perfused mice with EAE, following homogenisation and centrifugation on a Percoll gradient. Mononuclear cells (MNC) (2×10^6/ml) were stimulated for 4 h with PMA (10 ng/ml) and ionomycin (1 μg/ml) in the presence of brefeldin A (5 μg/ml). Cells were washed in PBS and re-suspended in 50 μL PBS with 1:1,000 LIVE/DEAD® Fixable Aqua Dead Cell Stain kit (Life Technologies) for 20 min. Surface stains for CD3 (145-2c11) (0.5 μl/10^6 cells), CD4 (RM4-5) (0.5 μl/10^6 cells) and γδ TCR (GL3) (1 μl/10^6 cells) (eBioscience) were added and cells were incubated for a further 20 mins. Cells were then fixed with 2% paraformaldehyde and washed in PBS twice, before being intracellularly stained for IL-17 or IFN-γ in permeabilization buffer (0.2% saponin in PBS + 1% FBS). Flow cytometric analysis of MNC was performed using a BD LSRFortessa™ (BD Biosciences) and analysed with FlowJo software. MNC were first gated on live $CD3^+$ T cells followed by CD4 expression, γδ TCR expression or cytokine production.

NLRP3 and NLRP1 activating mutation mice

Mice were backcrossed to C57BL/6 at least ten times. *Nlrp3A*^{350VneoR} mice were provided by Hal M. Hoffman, The University of California, San Diego, U.S.A.[44] and crossed with LysMCre mice (B6.1*29P2-Lyz2*$^{tm1(cre)Ifo/J}$. MCC950 was administered i.p. (20 mg/kg) every second day starting at day 4 after birth. Mice with an activating mutation in NLRP1, *Nlrp1a*^{Q593P} *were* generated on a C57BL/6 background as described previously[45] and administered MCC950 i.p. (20 mg/kg) every second day for 9 days. Blood was collected at the timepoints indicated for analysis of plasma cytokines by ELISA. IL-18 ELISA was performed as described by Westwell-Roper et al.[59] Experiments were performed under AEC Project 2013.011 and were approved by the Animal Ethics Committee of The Walter and Eliza Hall Institute of Medical Research.

Statistical analyses

Data are presented as average values ± S.E.M. from multiple individual experiments each carried out in triplicate or as average values ± S.D. from triplicate measurements in a representative experiment. Non-linear regression analysis of inhibitor vs. normalized response (variable slope) was performed using Prism Software (GraphPad). Statistical analysis was carried out using a nonparametric Mann-Whitney t test or an unpaired two-tailed t test using Prism Software (GraphPad). Data were were considered to be significant when $p \leq 0.05$ (*) or ≤ 0.005.

Supplementary Material

Refer to Web version on PubMed Central for supplementary material.

Acknowledgements

We would like to thanks Ana Kitanovic (German Center for Neurodegenerative Diseases) for image analysis in Fig. 3c.

References

1. Wen H, Miao EA, Ting JP. Mechanisms of NOD-like receptor-associated inflammasome activation. Immunity. 2013; 39:432–441. [PubMed: 24054327]
2. Schroder K, Tschopp J. The inflammasomes. Cell. 2010; 140:821–832. [PubMed: 20303873]
3. Latz E, Xiao TS, Stutz A. Activation and regulation of the inflammasomes. Nat Rev Immunol. 2013; 13:397–411. [PubMed: 23702978]
4. Lamkanfi M, Dixit VM. Mechanisms and functions of inflammasomes. Cell. 2014; 157:1013–1022. [PubMed: 24855941]
5. Masters SL, Simon A, Aksentijevich I, Kastner DL. Horror autoinflammaticus: the molecular pathophysiology of autoinflammatory disease (*). Annu Rev Immunol. 2009; 27:621–668. [PubMed: 19302049]
6. Wen H, Ting JP. O'Neill, LA A role for the NLRP3 inflammasome in metabolic diseases-did Warburg miss inflammation? Nat Immunol. 2012; 13:352–357. [PubMed: 22430788]
7. De Nardo D, De Nardo CM, Latz E. New Insights into Mechanisms Controlling the NLRP3 Inflammasome and Its Role in Lung Disease. Am J Pathol. 2014; 184:42–54. [PubMed: 24183846]
8. Szabo G, Csak T. Inflammasomes in liver diseases. J Hepatol. 2012; 57:642–654. [PubMed: 22634126]
9. Anders HJ, Muruve DA. The inflammasomes in kidney disease. J Am Soc Nephrol. 2011; 22:1007–1018. [PubMed: 21566058]
10. Youm YH, et al. Canonical Nlrp3 inflammasome links systemic low-grade inflammation to functional decline in aging. Cell Metab. 2013; 18:519–532. [PubMed: 24093676]
11. Masters SL, et al. Activation of the NLRP3 inflammasome by islet amyloid polypeptide provides a mechanism for enhanced IL-lbeta in type 2 diabetes. Nat Immunol. 2010; 11:897–904. [PubMed: 20835230]
12. Dinarello CA, van der Meer JW. Treating inflammation by blocking interleukin-1 in humans. Semin Immunol. 2013
13. Lamkanfi M, et al. Glyburide inhibits the Cryopyrin/Nalp3 inflammasome. J Cell Biol. 2009; 187:61–70. [PubMed: 19805629]
14. Coll RC, Robertson A, Butler M, Cooper M, O'Neill LA. The cytokine release inhibitory drug CRID3 targets ASC oligomerisation in the NLRP3 and AIM2 inflammasomes. PloS one. 2011; 6:e29539. [PubMed: 22216309]
15. Juliana C, et al. Anti-inflammatory compounds parthenolide and Bay 11-7082 are direct inhibitors of the inflammasome. J Biol Chem. 2010; 285:9792–9802. [PubMed: 20093358]
16. He Y, et al. 3,4-Methylenedioxy-beta-nitrostyrene Inhibits NLRP3 Inflammasome Activation by Blocking Assembly of the Inflammasome. J Biol Chem. 2014; 289:1142–1150. [PubMed: 24265316]
17. Ahn H, Kim J, Jeung EB, Lee GS. Dimethyl sulfoxide inhibits NLRP3 inflammasome activation. Immunobiology. 2013
18. Perregaux DG, et al. Identification and characterization of a novel class of interleukin-1 post-translational processing inhibitors. J Pharmacol Exp Ther. 2001; 299:187–197. [PubMed: 11561079]
19. Laliberte RE, et al. Glutathione s-transferase omega 1-1 is a target of cytokine release inhibitory drugs and may be responsible for their effect on interleukin-lbeta posttranslational processing. J Biol Chem. 2003; 278:16567–16578. [PubMed: 12624100]
20. Mariathasan S, et al. Cryopyrin activates the inflammasome in response to toxins and ATP. Nature. 2006; 440:228–232. [PubMed: 16407890]
21. Martinon F, Petrilli V, Mayor A, Tardivel A, Tschopp J. Gout-associated uric acid crystals activate the NALP3 inflammasome. Nature. 2006; 440:237–241. [PubMed: 16407889]
22. Gross O, et al. Inflammasome activators induce interleukin-lalpha secretion via distinct pathways with differential requirement for the protease function of caspase-1. Immunity. 2012; 36:388–400. [PubMed: 22444631]

23. Jin C, et al. NLRP3 inflammasome plays a critical role in the pathogenesis of hydroxyapatite-associated arthropathy. Proceedings of the National Academy of Sciences of the United States of America. 2011; 108:14867–14872. [PubMed: 21856950]
24. Netea MG, et al. Differential requirement for the activation of the inflammasome for processing and release of IL-lbeta in monocytes and macrophages. Blood. 2009; 113:2324–2335. [PubMed: 19104081]
25. Kayagaki N, et al. Non-canonical inflammasome activation targets caspase-11. Nature. 2011; 479:117–121. [PubMed: 22002608]
26. Kayagaki N, et al. Noncanonical inflammasome activation by intracellular LPS independent of *TLR4*. Science. 2013; 341:1246–1249. [PubMed: 23887873]
27. Broz P, von Moltke J, Jones JW, Vance RE, Monack DM. Differential requirement for Caspase-1 autoproteolysis in pathogen-induced cell death and cytokine processing. Cell Host Microbe. 2010; 8:471–483. [PubMed: 21147462]
28. Burckstummer T, et al. An orthogonal proteomic-genomic screen identifies AIM2 as a cytoplasmic DNA sensor for the inflammasome. Nat Immunol. 2009; 10:266–272. [PubMed: 19158679]
29. Hornung V, et al. AIM2 recognizes cytosolic dsDNA and forms a caspase-1-activating inflammasome with ASC. Nature. 2009; 458:514–518. [PubMed: 19158675]
30. Fernandes-Alnemri T, Yu JW, Datta P, Wu J, Alnemri ES. AIM2 activates the inflammasome and cell death in response to cytoplasmic DNA. Nature. 2009; 458:509–513. [PubMed: 19158676]
31. Roberts TL, et al. HIN-200 proteins regulate caspase activation in response to foreign cytoplasmic DNA. Science. 2009; 323:1057–1060. [PubMed: 19131592]
32. Kwok BH, Koh B, Ndubuisi MI, Elofsson M, Crews CM. The anti-inflammatory natural product parthenolide from the medicinal herb Feverfew directly binds to and inhibits IkappaB kinase. Chem Biol. 2001; 8:759–766. [PubMed: 11514225]
33. Hornung V, et al. Silica crystals and aluminum salts activate the NALP3 inflammasome through phagosomal destabilization. Nat Immunol. 2008; 9:847–856. [PubMed: 18604214]
34. Boyden ED, Dietrich WF. Nalplb controls mouse macrophage susceptibility to anthrax lethal toxin. Nat Genet. 2006; 38:240–244. [PubMed: 16429160]
35. Munoz-Planillo R, et al. K(+) efflux is the common trigger of NLRP3 inflammasome activation by bacterial toxins and particulate matter. Immunity. 2013; 38:1142–1153. [PubMed: 23809161]
36. Ashcroft FM. ATP-sensitive potassium channelopathies: focus on insulin secretion. The Journal of clinical investigation. 2005; 115:2047–2058. [PubMed: 16075046]
37. Petrilli V, et al. Activation of the NALP3 inflammasome is triggered by low intracellular potassium concentration. Cell death and differentiation. 2007; 14:1583–1589. [PubMed: 17599094]
38. Horng T. Calcium signaling and mitochondrial destabilization in the triggering of the NLRP3 inflammasome. Trends in immunology. 2014; 35:253–261. [PubMed: 24646829]
39. He Y, Franchi L, Nunez G. TLR agonists stimulate Nlrp3-dependent IL-lbeta production independently of the purinergic P2×7 receptor in dendritic cells and in vivo. Journal of immunology. 2013; 190:334–339.
40. Lalor SJ, et al. Caspase-1-processed cytokines IL-lbeta and IL-18 promote IL-17 production by gammadelta and CD4 T cells that mediate autoimmunity. Journal of immunology. 2011; 186:5738–5748.
41. Sutton C, Brereton C, Keogh B, Mills KH, Lavelle EC. A crucial role for interleukin (IL)-l in the induction of IL-17-producing T cells that mediate autoimmune encephalomyelitis. J Exp Med. 2006; 203:1685–1691. [PubMed: 16818675]
42. Sutton CE, et al. Interleukin-1 and IL-23 induce innate IL-17 production from gammadelta T cells, amplifying Thl7 responses and autoimmunity. Immunity. 2009; 31:331–341. [PubMed: 19682929]
43. Gris D, et al. NLRP3 plays a critical role in the development of experimental autoimmune encephalomyelitis by mediating Thl and Thl7 responses. Journal of immunology. 2010; 185:974–981.
44. Brydges SD, et al. Inflammasome-mediated disease animal models reveal roles for innate but not adaptive immunity. Immunity. 2009; 30:875–887. [PubMed: 19501000]

45. Masters SL, et al. NLRP1 inflammasome activation induces pyroptosis of hematopoietic progenitor cells. Immunity. 2012; 37:1009–1023. [PubMed: 23219391]
46. Hoffman HM, Mueller JL, Broide DH, Wanderer AA, Kolodner RD. Mutation of a new gene encoding a putative pyrin-like protein causes familial cold autoinflammatory syndrome and Muckle-Wells syndrome. Nature genetics. 2001; 29:301–305. [PubMed: 11687797]
47. Gattorno M, et al. Pattern of interleukin-lbeta secretion in response to lipopolysaccharide and ATP before and after interleukin-1 blockade in patients with CIAS1 mutations. Arthritis Rheum. 2007; 56:3138–3148. [PubMed: 17763411]
48. Lee GS, et al. The calcium-sensing receptor regulates the NLRP3 inflammasome through Ca2+ and cAMP. Nature. 2012; 492:123–127. [PubMed: 23143333]
49. Bauernfeind F, et al. Cutting edge: reactive oxygen species inhibitors block priming, but not activation, of the NLRP3 inflammasome. Journal of immunology. 2011; 187:613–617.
50. Brydges SD, et al. Divergence of IL-1, IL-18, and cell death in NLRP3 inflammasomopathies. The Journal of clinical investigation. 2013; 123:4695–4705. [PubMed: 24084736]
51. Lopez-Castejon G, Pelegrin P. Current status of inflammasome blockers as antiinflammatory drugs. Expert opinion on investigational drugs. 2012; 21:995–1007. [PubMed: 22612568]
52. Fautrel B. Economic benefits of optimizing anchor therapy for rheumatoid arthritis. Rheumatology (Oxford). 2012; 51(Suppl 4):iv21–iv26. [PubMed: 22685272]
53. Urban FJ, et al. Novel synthesis of 1-(1,2,3,5,6,7-hexahydro-s-indacen-4-yl)-3-[4-(1-hydroxy-1-methyl-ethyl)-furan-2-sulfonyl]urea, an anti-inflammatory agent. Synthetic Commun. 2003; 33:2029–2043.
54. Kuida K, et al. Altered cytokine export and apoptosis in mice deficient in interleukin-1 beta converting enzyme. Science. 1995; 267:2000–2003. [PubMed: 7535475]
55. Wang S, et al. Murine caspase-11, an ICE-interacting protease, is essential for the activation of ICE. Cell. 1998; 92:501–509. [PubMed: 9491891]
56. Hett EC, et al. Chemical genetics reveals a kinase-independent role for protein kinase R in pyroptosis. Nature chemical biology. 2013; 9:398–405.
57. Croker DE, et al. C5a2 can modulate ERK1/2 signaling in macrophages via heteromer formation with C5a1 and beta-arrestin recruitment. Immunology and cell biology. 2014; 92:631–639. [PubMed: 24777312]
58. Sester DP, et al. A novel flow cytometric method to assess inflammasome formation. Journal of immunology. 2015; 194:455–462.
59. Westwell-Roper C, Dunne A, Kim ML, Verchere CB, Masters SL. Activating the NLRP3 inflammasome using the amyloidogenic peptide IAPP. Methods in molecular biology. 2013; 1040:9–18. [PubMed: 23852593]

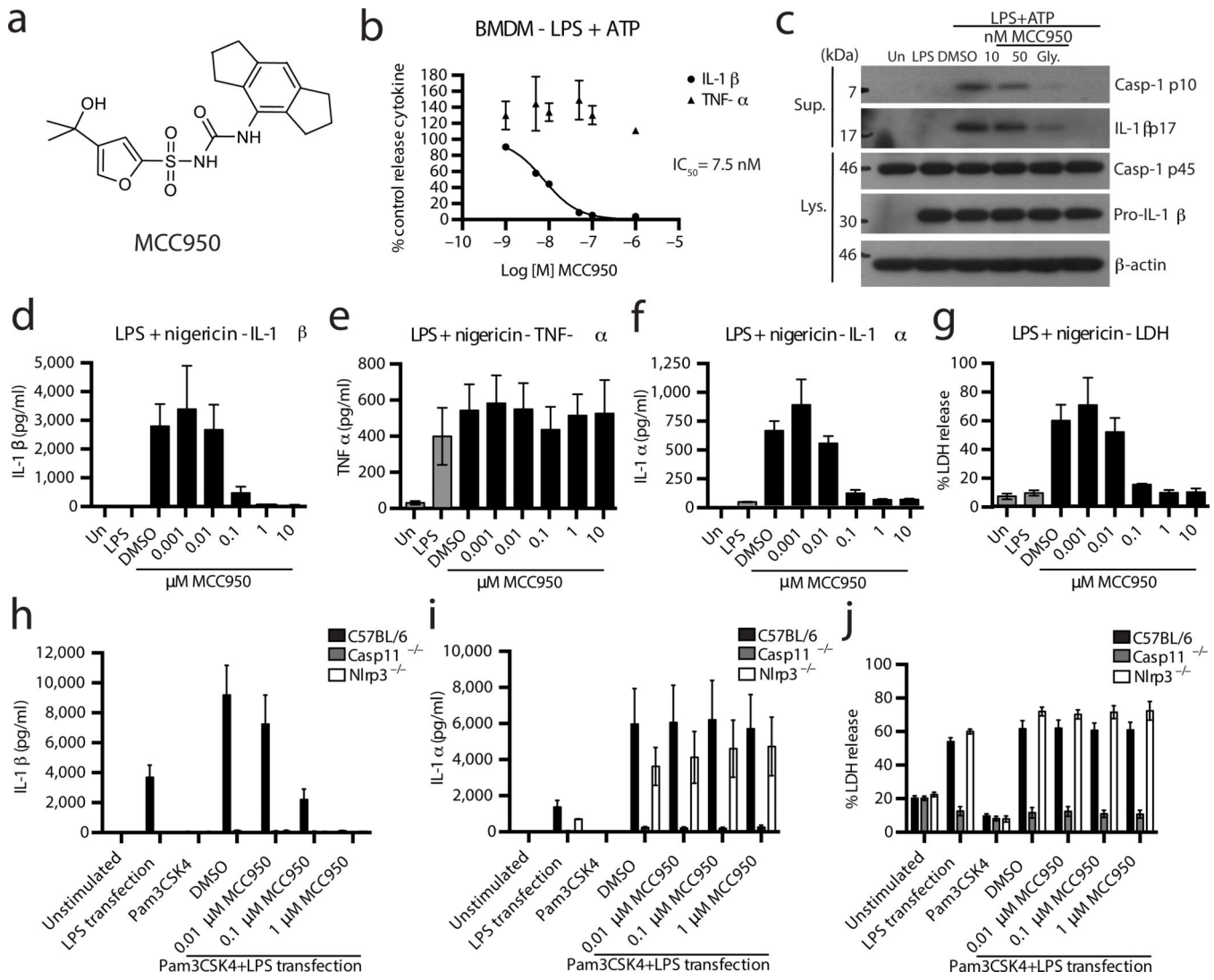

Figure 1. MCC950 inhibits NLRP3 inflammasome activation in response to canonical and non-canonical NLRP3 stimuli

(**a**) MCC950 structure. (**b**) Production of IL-1β and TNF-α from BMDM stimulated with LPS and ATP and treated with MCC950 (1-1,000 nM) measured by ELISA. Cytokine level is normalized to DMSO control treated cells. Data are expressed as mean ± S.E.M. of six independent experiments carried out in triplicate. Non-linear regression analysis was performed and Log [M] MCC950 vs. normalized response (variable slope) curve is presented. (**c**) Western blots of cell lysates and supernatants from BMDM stimulated with LPS and ATP and treated with MCC950 or glyburide. These results are representative of five independent experiments. (**d–g**) Production of IL-1β, TNF-α, IL-1α and LDH from BMDM stimulated with LPS and nigericin and treated with MCC950 as measured by ELISA (**d–f**) and LDH assay (**g**). Data are expressed as mean ± S.E.M. of three independent experiments carried out in triplicate. (**h–j**) Production of IL-1β, IL-1α and LDH from BMDM from the indicated genotypes stimulated with Pam3CSK4 and transfected LPS and treated with MCC950 as measured by ELISA (**h,i**) and LDH assay (**j**). Data are expressed as

mean ± S.E.M. of three (*Nlrp3*$^{-/-}$), four (*casp11*$^{-/-}$) or six (C57BL/6) independent experiments.

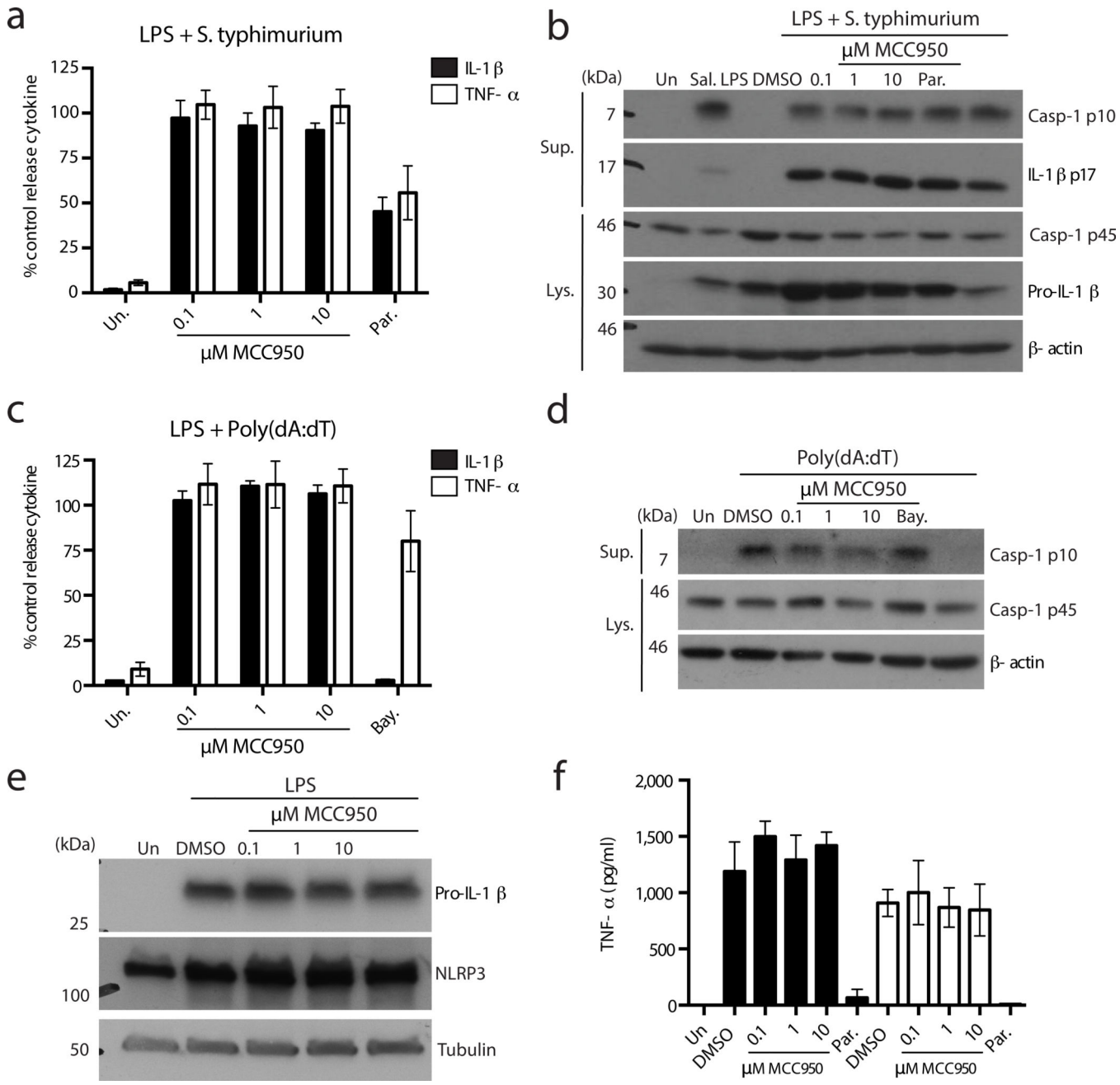

Figure 2. MCC950 does not inhibit NLRC4, AIM2, TLR signalling or priming of NLRP3

(**a**) Production of IL-1β and TNF-α from BMDM stimulated with LPS and *S. typhimurium* and treated with MCC950 and parthenolide measured by ELISA. Cytokine level is normalized to DMSO control treated cells. Data are expressed as mean ± S.E.M. of four independent experiments carried out in triplicate. (**b**) Western blots of cell lysates and supernatants from BMDM stimulated with LPS and *S. typhimurium* and treated with MCC950 and parthenolide. These results are representative of four independent experiments. (**c**) Production of IL-1β and TNF-α from BMDM stimulated with LPS and transfected Poly(dA:dT) and treated with MCC950 and Bayer compound measured by

ELISA. Cytokine level is normalized to DMSO control treated cells. Data are expressed as mean ± S.E.M. of five independent experiments carried out in triplicate. (**d**) Western blots of cell lysates and supernatants from BMDM stimulated with LPS and transfected Poly(dA:dT) and treated with MCC950 and Bayer compound. These results are representative of two independent experiments. (**e**) Western blots of cell lysates from BMDM treated with MCC950 and stimulated with LPS (4 h). These results are representative of three independent experiments. (**f**) Production of TNF-α from BMDM treated with MCC950 and parthenolide and stimulated with LPS or Poly(A:U) measured by ELISA. Data shown represent mean cytokine level ± S.D. from triplicate determinations and are representative of three independent experiments.

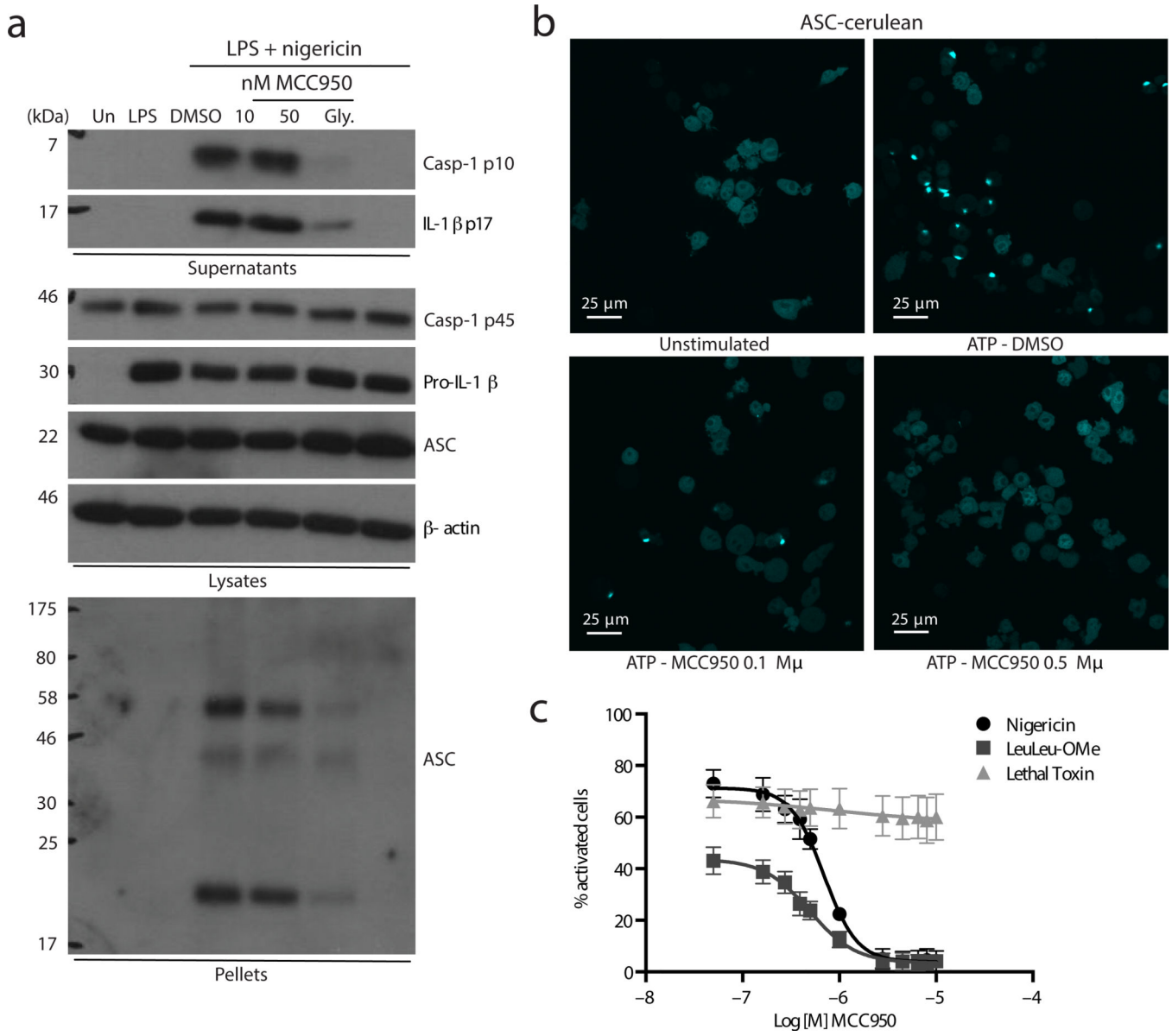

Figure 3. MCC950 blocks NLRP3 dependent ASC oligomerization

(**a**) Western blots of cell lysates, supernatants and cross-linked cytosolic pellets from BMDM stimulated with LPS and nigericin and treated with MCC950 and parthenolide. These results are representative of three independent experiments. (**b**) Live cell imaging of ASC-cerulean cells treated with MCC950 and stimulated with ATP. At least five different images were taken of each condition at an original magnification of ×40. Results are representative of three independent experiments. (**c**) The percentage of ASC-cerulean cells containing an ASC speck after treatment with MCC950 (0.05-10 µM) and stimulation with nigericin, LeuLeu-Ome or lethal toxin. Data shown represent the mean ± S.D. from triplicate measurements.

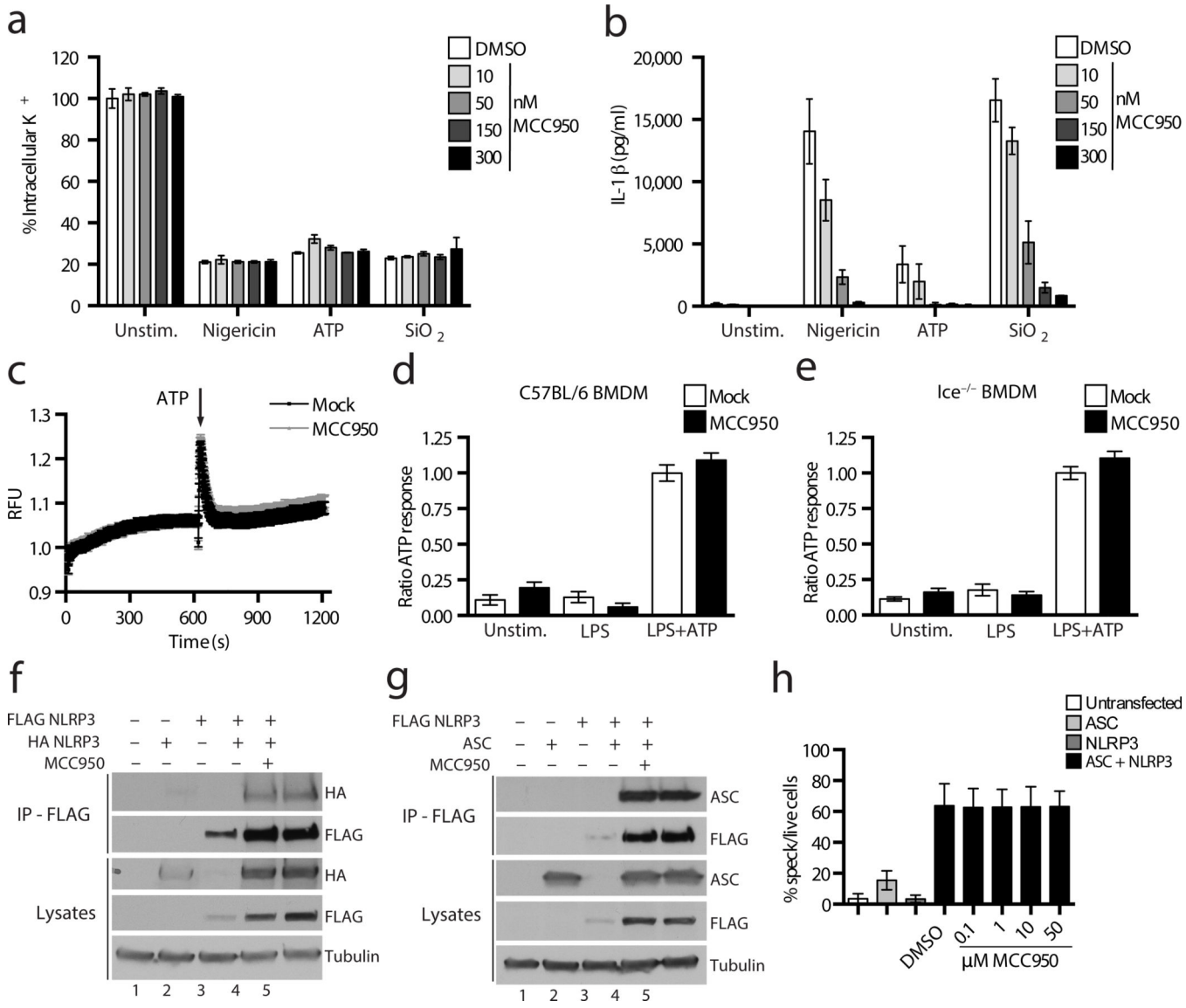

Figure 4. MCC950 does not block K^+ efflux, Ca^{2+} flux or direct NLRP3 and ASC interactions

(**a**) The relative level of intracellular K^+ determined by ICP-OES in *Nlrp3*$^{-/-}$ BMDM stimulated with LPS and nigericin, ATP and SiO_2 and treated with MCC950. (**b**) IL-1β production from C57BL/6 BMDM stimulated with LPS and nigericin, ATP and SiO_2 measured by ELISA. (**a-b**) Data are presented as mean ± S.D. from triplicate measurements and are representative of three independent experiments. (**c**) A trace showing ATP induced Ca^{2+} flux was measured using the FLIPR^{TETRA} system in C57BL/6 BMDM stimulated with LPS and treated with MCC950. The results are representative of three independent experiments. (**d,e**) The relative response to ATP induced Ca^{2+} flux in C57BL/6 (**d**) and *Ice*$^{-/-}$ (**e**) BMDM stimulated with LPS and treated with MCC950 as measured using the FLIPR^{TETRA} system. Data are presented as mean ± S.E.M. and are representative of three independent experiments. (**f,g**) Western blots of cell lysates and FLAG-immunoprecipitation samples from HEK-293T cells transfected with FLAG-NLRP3, HA-NLRP3, ASC or empty vector plasmids as indicated and treated with MCC950. These results presented are

representative of three independent experiments. (**h**) The percentage of ASC speck containing live HEK-293T cells transfected with GFP-ASC and NLRP3-mCherry plasmids as indicated, treated with MCC950. and analysed by FACS. Data is presented as mean ± S.E.M. from three independent experiments each carried out in triplicate.

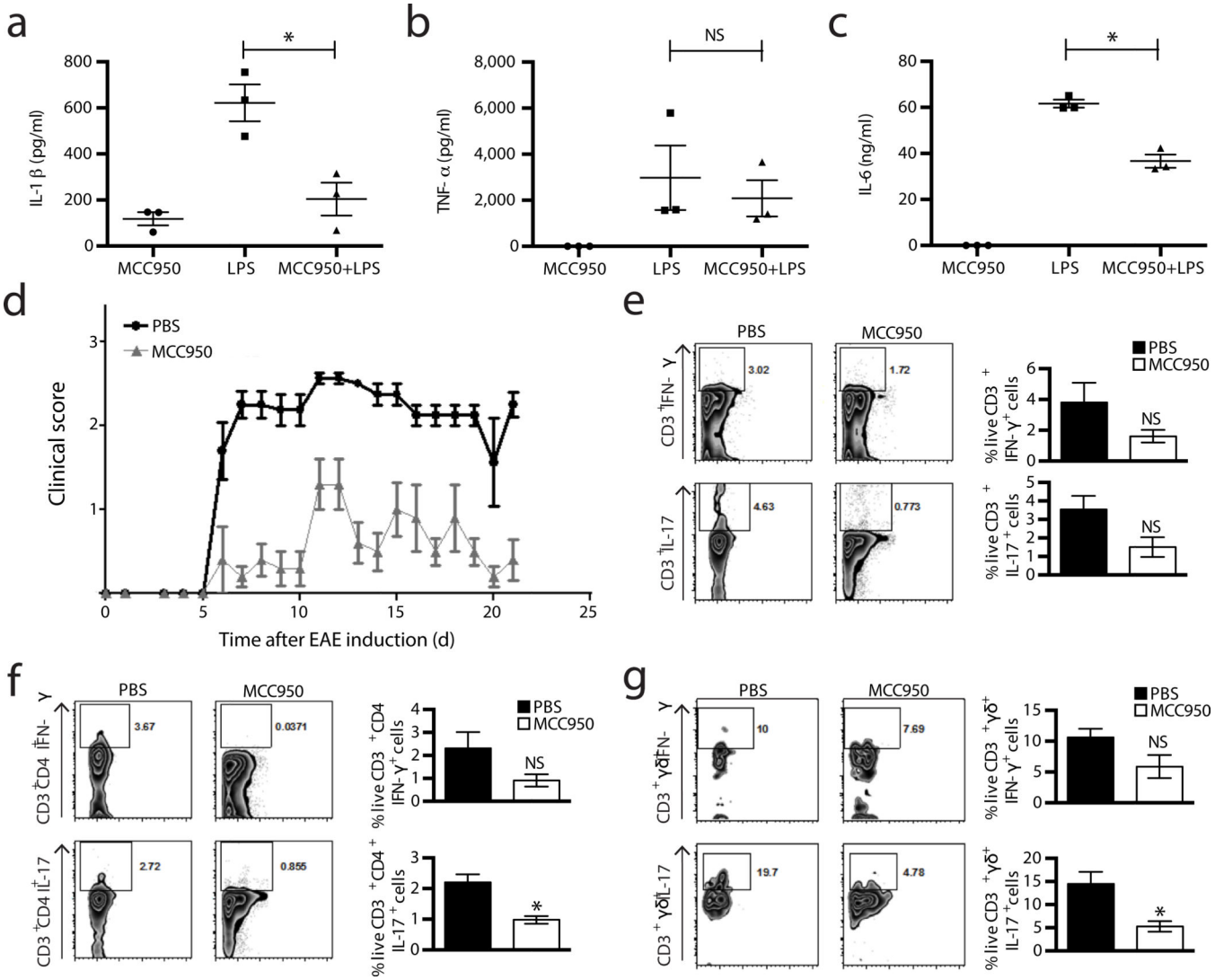

Figure 5. MCC950 is active *in vivo and* treatment of mice with MCC950 attenuates EAE

(**a–c**) Serum levels of IL-1β (**a**), TNF-α (**b**) and IL-6 (**c**) measured by ELISA from C57BL/6 mice pre-treated with MCC950 or vehicle control, 2 h post i.p. LPS injection. Data shown are mean values ± S.D. n=3, *$P \leq 0.05$ by Mann-Whitney test. (**d**) Clinical scores after EAE induction from C57BL/6 treated with PBS or MCC950. Mean ± S.D. n=6.(**e–g**) Representative dot plots from five mice and mean percentages ± S.D. of live IL-17 and IFN-γ secreting $CD3^+$ T cells (**e**), $CD3^+$ $CD4^+$ T cells (**f**) or $CD3^+$ γδ TCR^+ cells (**g**) from brain mononuclear cells isolated on day 22 post EAE induction in C57BL/6 mice treated with PBS or MCC950 are shown. n=5, *$P \leq 0.05$ by Mann-Whitney test.

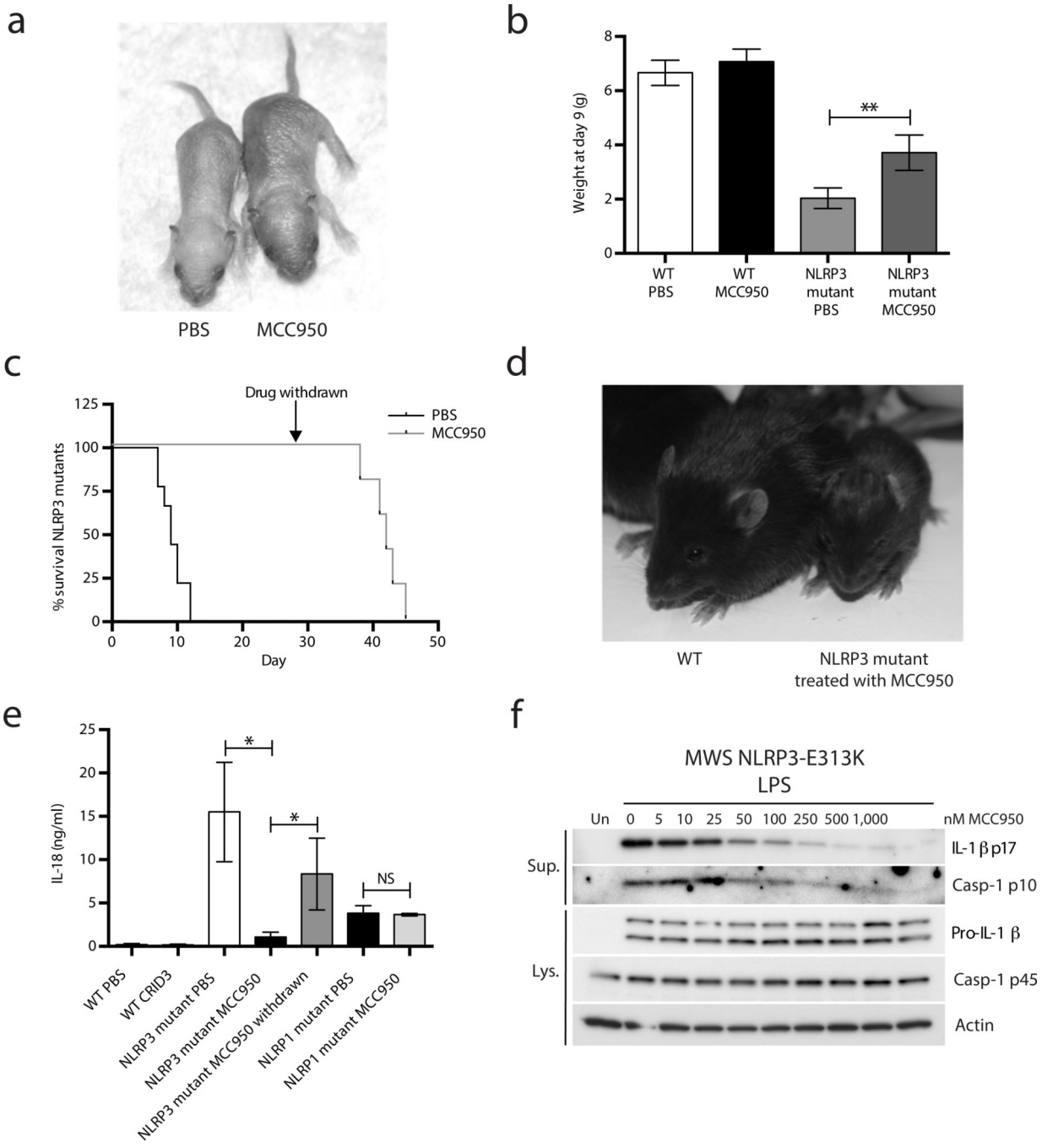

Figure 6. MCC950 inhibits NLRP3 activation in a mouse model of MWS and in MWS PBMC *ex vivo*

(**a**) *Nlrp3A*^{350VneoR} crossed with LysMCre mice (NLRP3 mutant) treated with PBS or MCC950 at day 9. (**b**) Weight at day 9. Mean ± S.D. WT PBS and WT MCC950 both n=4, NLRP3 mutant PBS n=3 and NLRP3 mutant MCC950 n=6. **$P \leq 0.005$ by unpaired two-tailed t-test. (**c**) Survival of NLRP3 mutant mice treated with PBS or MCC950 up to day 45 (MCC950 withdrawn at day 28). MCC950 group n=5, PBS group n=9. (**d**) WT and NLRP3 mutant mice on day 17. (**e**) Plasma IL-18 concentrations as measured by ELISA at day 9,

and again for NLRP3 mutant mice 14 days after drug withdrawal. WT PBS and WT MCC950 both *n*=4, NLRP3 mutant PBS *n*=5 and NLRP3 mutant MCC950 and withdrawal both *n*=4. *NLRP1a*^{Q593P} mice (NLRP1 mutant) PBS and MCC950 both *n*=3. Data shown are mean ± S.D. * $P \leq 0.05$ by Mann-Whitney test. (**f**) Western blots of cell lysates and supernatants from PBMC isolated from an individual with MWS (mutation E313K) stimulated with LPS and treated with MCC950.